 doi:10.20944/preprints201905.0096.v1

Late-transition constraints in a geometric model for dark energy

Abraão J. S. Capistrano*
Applied physics graduation program, Federal University of Latin-American Integration, 85867-670, P.o.b: 2123, Foz do Iguassu-PR, Brazil.
Casimiro Montenegro Filho Astronomy Center, Itaipu Technological Park, 85867-900, Foz do Iguassu-PR, Brazil.
(Dated: May 6, 2019)

In a geometric model for dark energy, the Hubble parameter as a function of redshift is modified by the presence of a new term originated from the extrinsic curvature. We investigate a late-transition redshift constrained with the latest datasets on the Cosmic Microwave Background (CBM), Baryon Acoustic Oscillations (BAO), the Pantheon Supernovae type Ia and the Hubble parameter data with redshift ranging from $0.01 < z < 2.3$. Performing the Aikake Information Criterion (AIC) to ascertain the viability of the model from Jeffreys' scale, we apply a joint likelihood analysis with the Markov Chain Monte Carlo (MCMC) method and find that the present model is in very good agreement with observations with a close statistical equivalence with the background ΛCDM cosmology at 1-σ level. In addition, we apply the Bayesian Information Criterion (BIC) to the statistics and we find similar results as compared to AIC. Both tests indicate that mild deviations from ΛCDM model are allowed, showing no evidence for phantom behaviour.

I. INTRODUCTION

After compelling evidences, the accelerated expansion of the universe is constituting one of the greatest challenges for theoretical physics and cosmology. In the last 20 years, the main proposal for the explanation of the current accelerated regime is the well known dark energy hypothesis, consisting in a sort of a cosmological energy with negative pressure that drives the universe to speed up. In that sense, the simplest model is the popular ΛCDM model. Even though its success, the main components of this model remain in the lack of a fundamental understanding, since the Cosmological constant Λ and the Cold dark matter (CDM) are problems of their own [1–7]. These particular problems motivated the investigation of new possibilities for the explanation of the accelerated phase of the universe.

The overall feeling consists in constraining both cosmological and model parameters to grasp an underlying understanding of the fundamental physics on the acceleration expansion problem, whether such component is a time-independent (the cosmological constant) or possesses a dynamical origin. To this matter, an equation of state turns a fundamental cornerstone to confront a model to observational data. For instance, the related dark energy equation of state (EOs) presents a negative fluid parameter, $w = -1$ [8] and competitive models must comply to mild deviations with accordance with the latest indications.

One of the alternative routes of investigation is being explored by the possibility that the universe might be embedded in extra dimensions. Most of these models have been Kaluza-Klein or/and string inspired, such as, for instance, the seminal works of the Arkani-Hamed, Dvali and Dimopolous (ADD) model [9], the Randall-sundrum model [10, 11] and the Dvali-Gabadadze-Porrati model (DPG)[12]. In all those models and variants, the embedding was a rising issue not completed worked as a theoretical background since its generally fixed to a boundary and specific conditions are needed to obtain its dynamics. Till then, several authors explored embedding as a promising mathematical structure for a physical theory with the embedding equations as a fundamental mathematical guide [13–25].

Using the embedding framework, this paper aims at investigating in a late redshift transition ($z \geq 1$) on how the cosmological parameters are accommodated in the present model under this assumption, focusing on the current matter density Ω_{m0}, the physical baryon density $100\Omega_b h^2$ and the dimensionless Hubble parameter h. The study of late-transitions have been focus of active research since it may be possible that the accelerated regime may be its origins at redshift $z \gtrsim 1$. This inflicts an interesting non-standard situation departing from the non-dynamical ΛCDM cosmology since at high redshifts the constraints are hitherto weaker [26–33].

We perform the Markov Chain Monte Carlo (MCMC) sample technique with a modified code from the original basis published in [34, 35] as a tool for analysing fit-to-data. Hence, the joint likelihood is performed from the latest data on Cosmic Microwave Background (CMB) Planck 2015 data [8], the largest dataset Pantheon SnIa [36] with redshift ranging from $0.01 < z < 2.3$, the Hubble parameter as a function of redshift ($H(z)$)[37–42] and Baryonic Acoustic Oscillations (BAO) from points of the joint surveys 6dFGS [43], SDDS [44], BOSS CMASS [45], WiggleZ [46], MSG[47] and BOSS DR12 [48].

The paper is organized as follows: in the second section, we make a brief mathematical review on the theoretical framework and its resulting cosmological model. The third section presents the outcomes and discussions from the comparison of the present model to the models as ΛCDM, quintessense model (wCDM)[49, 50] and Chevallier-Polarski-Linder (CPL) [51, 52]. A analysis on

* abraao.capistrano@unila.edu.br

Preprints (www.preprints.org) | NOT PEER-REVIEWED | Posted: 8 May 2019 doi:10.20944/preprints201905.0096.v1

the statistical tension between the models is made by using the Akaike Information Criterion (AIC)[53] and Bayesian Information Criterion (BIC) [54] on the confidence regions of the resulting contours. In the final section, we conclude with our remarks and future prospects.

II. THE MODEL

The gravitational action functional in the presence of confined matter field on a four-dimensional embedded space with thickness l embedded in a D-dimensional ambient space (bulk) has the form

$$S = -\frac{1}{2\kappa_D^2}\int \sqrt{|\mathcal{G}|}\mathcal{R}d^Dx - \int \sqrt{|\mathcal{G}|}\mathcal{L}_m^* d^Dx \ , \quad (1)$$

where κ_D^2 is the fundamental energy scale on the embedded space, $\mathcal{R}$ denotes de Ricci scalar of the bulk and $\mathcal{L}_m^*$ is the confined matter lagrangian. In this model, the matter energy momentum tensor occupies a finite hypervolume with constant radius l along the extra-dimensions. The variation of Einstein-Hilbert action in Eq.(1) with respect to the bulk metric $\mathcal{G}_{AB}$ leads to the Einstein equations for the bulk

$$\mathcal{R}_{AB} - \frac{1}{2}\mathcal{G}_{AB} = \alpha^\star \mathcal{T}_{AB} \ , \quad (2)$$

where $\alpha^\star$ is energy scale parameter and $\mathcal{T}_{AB}$ is the energy-momentum tensor for the bulk [15, 16, 19]. To generate a thick embedded space-time is important to perturb the related background and it should be done in accordance with the confinement hypothesis of gauge interactions that depends only on the four-dimensionality of the space-time [55, 56] in accordance with current phenomenology [57].

Nash's original embedding theorem [58] used a flat D-dimensional Euclidean space, later generalized to any Riemannian manifold including non-positive signatures by Greene [59] with independent orthogonal perturbations. It guarantees that the embedded geometry remains smooth (differentiable) after perturbations. With all these concepts, let us consider a Riemannian manifold V_4 with a non-perturbed metric $\bar{g}_{\mu\nu}$ being locally and isometrically embedded in a n-dimensional Riemannian manifold V_n given by a differentiable and regular map $\mathcal{X} : V_4 \to V_n$ satisfying the embedding equations

$$\mathcal{X}^A_{,\mu}\mathcal{X}^B_{,\nu}\mathcal{G}_{AB} = \ \bar{g}_{\mu\nu} \quad (3)$$

$$\mathcal{X}^A_{,\mu}\bar{\eta}^B_a\mathcal{G}_{AB} = \ 0 \quad (4)$$

$$\bar{\eta}^A_a\bar{\eta}^B_b\mathcal{G}_{AB} = \ \bar{g}_{ab} \ . \quad (5)$$

where we have denoted by $\mathcal{G}_{AB}$ the metric components of V_n in arbitrary coordinates, $\bar{\eta}$ denotes a non-perturbed unit vector field orthogonal to V_4. Concerning notation, capital Latin indices run from 1 to n. Small case Latin indices refer to the only one extra dimension considered. All Greek indices refer to the embedded space-time counting from 1 to 4. These set of equations represent the isometry condition Eq.(3), orthogonality between the embedding coordinates $\mathcal{X}$ and $\bar{\eta}$ in Eq.(4), and also, the vector normalization $\bar{\eta}$ and $\bar{g}_{ab} = \epsilon_a\delta_{ab}$ with $\epsilon_a = \pm 1$ in which the signs represent the signatures of the extra-dimensions. Hence, the integration of the system of equations Eqs.(3), (4) and (5) assures the configuration of the embedding map $\mathcal{X}$.

The second fundamental form, or more commonly, the non-perturbed extrinsic curvature $\bar{k}_{\mu\nu}$ of V_4 is by definition the projection of the variation of $\bar{\eta}$ onto the tangent plane :

$$\bar{k}_{\mu\nu} = -\mathcal{X}^A_{,\mu}\bar{\eta}^B_{,\nu}\mathcal{G}_{AB} = \mathcal{X}^A_{,\mu\nu}\bar{\eta}^B\mathcal{G}_{AB} \ , \quad (6)$$

where the comma denotes the ordinary derivative.

To obtain the embedded four-dimensional equations, one can take Eq.(2) written in the Gaussian frame embedding veilbein $\{\mathcal{X}^A_\mu, \eta^A_a\}$. This reference frame is composed by a regular and differentiable coordinate $\{\mathcal{X}^A_\mu\}$ and a unitary normal vector $\{\eta^A_a\}$. Accordingly, they define the basis of the embedded geometry and one can obtain the embedded four-dimensional field equations

$$R_{\mu\nu} - \frac{1}{2}Rg_{\mu\nu} - Q_{\mu\nu} = -8\pi G T_{\mu\nu} \ , \quad (7)$$

$$k^{\ \rho}_{\mu;\rho} - h_{,\mu} = 0 \ , \quad (8)$$

where the semi-colon denotes a covariant derivative. The $T_{\mu\nu}$ tensor is the four-dimensional energy-momentum tensor of a perfect fluid, expressed in co-moving coordinates as

$$T_{\mu\nu} = (p+\rho)U_\mu U_\nu + p\ g_{\mu\nu}, \quad U_\mu = \delta^4_\mu \ ,$$

where U_μ is the co-moving four-velocity.

Differently what happens to the usual general Relativity framework, the embedding between space-times leads to the appearance of the extrinsic terms. The deformation tensor $Q_{\mu\nu}$ is a geometrical term given by

$$Q_{\mu\nu} = g^{\rho\sigma}k_{\mu\rho}k_{\nu\sigma} - k_{\mu\nu}H - \frac{1}{2}\left(K^2 - h^2\right)g_{\mu\nu} \ , \quad (9)$$

where we denote $h = g^{\mu\nu}k_{\mu\nu}$ and $h^2 = h.h$ is the mean curvature. The term $K^2 = k^{\mu\nu}k_{\mu\nu}$ is the Gaussian curvature. It follows that $Q_{\mu\nu}$ is conserved in the sense of Noether's theorem

$$Q^{\mu\nu}{}_{;\nu} = 0 \ . \quad (10)$$

Using spatially flat Friedman-Lemaître-Robertson-Walker (FLRW) metric, one obtains a solution of Eq.(8) that is given by

$$k_{ij} = \frac{b}{a^2}g_{ij}, \quad i,j = 1,2,3, \quad k_{44} = \frac{-1}{\dot{a}}\frac{d}{dt}\frac{b}{a},$$

where the $a = a(t)$ is the usual expansion parameter and $b(t) = k_{11}$ is the bending function that is function of time.

Preprints (www.preprints.org) | NOT PEER-REVIEWED | Posted: 8 May 2019 doi:10.20944/preprints201905.0096.v1

The dot symbol denotes an ordinary time derivative.

Denoting the usual Hubble parameter by $H = \dot{a}/a$ and the extrinsic parameter $B = \dot{b}/b$, one obtains the following quantities

$$k_{44} = -\frac{b}{a^2}(\frac{B}{H} - 1), \tag{11}$$

$$K^2 = \frac{b^2}{a^4}\left(\frac{B^2}{H^2} - 2\frac{B}{H} + 4\right), \quad h = \frac{b}{a^2}(\frac{B}{H} + 2) \tag{12}$$

$$Q_{ij} = \frac{b^2}{a^4}\left(2\frac{B}{H} - 1\right) g_{ij}, \; Q_{44} = -\frac{3b^2}{a^4}, \tag{13}$$

$$Q = -(K^2 - h^2) = \frac{6b^2}{a^4}\frac{B}{H}\,, \tag{14}$$

where in Eq.(13), we have denoted $i, j = 1..3$, with no sum in indices. Moreover, the dynamics equations of the extrinsic curvature are complete in five-dimensions by the Einstein-Gupta equations [19, 60] in a form

$$\mathcal{F}_{\mu\nu} = 0\,, \tag{15}$$

where they are defined as a copy (concerning its structure) of the usual Riemannian geometry. Hence, once can define a "f-Riemann tensor"

$$\mathcal{F}_{\nu\alpha\lambda\mu} = \partial_\alpha \Upsilon_{\mu\lambda\nu} - \partial_\lambda \Upsilon_{\mu\alpha\nu} + \Upsilon_{\alpha\sigma\mu}\Upsilon^{\sigma}_{\lambda\nu} - \Upsilon_{\lambda\sigma\mu}\Upsilon^{\sigma}_{\alpha\nu}\,,$$
$$\Upsilon_{\mu\nu\sigma} = \frac{1}{2}\left(\partial_\mu f_{\sigma\nu} + \partial_\nu f_{\sigma\mu} - \partial_\sigma f_{\mu\nu}\right) \quad ,$$
$$\Upsilon_{\mu\nu}{}^{\lambda} = f^{\lambda\sigma}\,\Upsilon_{\mu\nu\sigma}.$$

that were constructed from a "connection" associated with $k_{\mu\nu}$ and

$$f_{\mu\nu} = \frac{2}{K}k_{\mu\nu}, \;\text{ and }\; f^{\mu\nu} = \frac{2}{K}k^{\mu\nu}\,, \tag{16}$$

in such a way that the normalization condition $f^{\mu\rho}f_{\rho\nu} = \delta^{\mu}_{\nu}$ applies. Thus, taking flat Friedman metric in Eq.(15), and with the results from Eqs.(7), (8) and (10), one obtains the Friedman equation modified by the extrinsic curvature as

$$\left(\frac{\dot{a}}{a}\right)^2 = \frac{8}{3}\pi G\rho + \alpha_0 a^{2\beta_0 - 4}e^{\gamma^{\pm}(t)}\,, \tag{17}$$

where α_0 denotes an integration constant and its value is set to 1 without loss of generality. Concerning the total energy ρ, we denote $\rho = \rho_{mat} + \rho_{rad}$, which are the matter and radiation energy densities. The γ-exponent in the exponential function in Eq.(17) is defined as $\gamma^{\pm}(t) = \pm\sqrt{|4\eta_0 a^4 - 3|} \mp \sqrt{3}\arctan\left(\frac{\sqrt{3}}{3}\sqrt{|4\eta_0 a^4 - 3|}\right)$. The parameter β_0 inflicts on the magnitude of the deceleration parameter $q(z)$ in function of the redshift z and the parameter η_0 measures the width of the transition phase redshift z_t from a decelerating to accelerating regime. In this work, we investigate late-transition redshift $z_t = 1$ when $\eta_0 = 0$, that leads to $\gamma(t) = \gamma_0 = \exp[(1 - \frac{\pi}{4})\sqrt{3}]$.

III. OBSERVATIONAL CONSTRAINTS: ANALYSIS AND RESULTS

A. Cosmological data

The methodology used in this paper relies on the Markov Chain Monte Carlo (MCMC) sample technique with Mathematica code modified from the original one [35] as a tool for analysing the background data. We perform our analysis using the joint likelihood of kinematical probes as of the CMB Planck 2015 data [8], Pantheon SnIa [36], the Hubble parameter as a function of redshift ($H(z)$) [37–42] and Baryonic Acoustic Oscillations (BAO) from points of the joint surveys 6dFGS [43], SDDS [44], BOSS CMASS [45], WiggleZ [46], MSG[47] and BOSS DR12 [48].

To apply our χ^2-statistics, we extract the data points from Pantheon set, CMB, BAO and Hubble parameter, with the amount of 1048, 3, 9 and 36 data points, respectively, with a total of 1096 data points. The parameters to vary were $\{\Omega_{m0}, 100\Omega_b h^2, h, \beta_0\}$ which denotes the current matter content, the physical baryon content, dimensionless Hubble parameter and the β_0-parameter. Concerning the β_0-parameter, we adopt for convenience of interpretation the fluid correspondence which is given by the relation

$$4 - 2\beta_0 = 3(1 + w)\,, \tag{18}$$

where w is a dimensionless parameter of the fluid equation of state $w = \frac{p}{\rho}$ [61] as a ratio between its pressure p and density ρ. Accordingly, the values of β_0 runs from 1.5 to 3 which means roughly $-1/3 \leq w \leq -1.5$, i.e, in fluid context, varying from quintessence to phantom fluids. The ΛCDM model corresponds to $w = -1$ or, equivalently, $\beta_0 = 2$.

To start with, we use the background parameter vectors $\{\Omega_{m0}, 100\Omega_b h^2, h, \beta_0\}$ which the adopted priors were $\{(0.001, 1), (0.001, 0.08), (0.4, 1), (1.9, 3)\}$, respectively. The CMB temperature we adopt the value $T_{cmb} = 2.7255K$. Moreover, the joint analysis was implemented by the product of the particular likelihoods $\mathcal{L}$ for each data set

$$\mathcal{L}_{tot} = \mathcal{L}_{Pantheon}.\mathcal{L}_{BAO}.\mathcal{L}_{CMB}.\mathcal{L}_{H(z)} \tag{19}$$

and the sum of individual χ^2 to get the related total χ^2

$$\chi^2_{tot} = \chi^2_{Pantheon} + \chi^2_{BAO} + \chi^2_{CMB} + \chi^2_{H(z)}\,. \tag{20}$$

The adopted values for the $H(z)$ data can be found in Table 1 of the ref.[35].

In order to make a proper description of the evolution of the density parameters, we must use the modified Friedman equation in a more appropriate form. Using Eq.(17), we can write Friedman equations as

$$H(z) = H_0\sqrt{\Omega_m(z) + \Omega_{rad}(z) + \Omega_{ext}(z)}\,, \tag{21}$$

Preprints (www.preprints.org) | NOT PEER-REVIEWED | Posted: 8 May 2019 doi:10.20944/preprints201905.0096.v1

TABLE I. A summary of best-fit values background parameters calculated by using MCMC chains with the main parameters and resulting χ^2 values. The χ^2_{min} denotes the χ^2 best-fit value from MCMC and χ^2_{tot} refers to the value of the total χ^2 from minimizing all data. For the sake of convenience, we refer the present model in this paper as β-model as shown below.

Model	Ω_{m0}	$\Omega_{b0}h^2$	h	DE parameters	χ^2_{min}	χ^2_{tot}
ΛCDM	0.3154± 0.0061	0.0222± 0.0001	0.6728± 0.0048	$w=-1$	1809.67	1809.75
wCDM	0.3163± 0.0081	0.0223± 0.0015	0.6717± 0.0074	w=-0.9927± 0.0268	1809.81	1809.75
CPL	0.3143± 0.0061	0.0223± 0.0001	0.6751± 0.0004	w=-0.9998± 0.0008 wa=-0.0166± 0.008	1809.69	1809.75
β-model	0.3127± 0.0079	0.0222± 0.0001	0.6761± 0.0085	β_0=2.0209± 0.05280	1809.60	1809.80

TABLE II. A summary of mean values of background parameters calculated by using MCMC chains with the main parameters.

Model	Ω_{m0}	$\Omega_{b0}h^2$	h	DE parameters
ΛCDM	0.3179± 0.0065	0.0223± 0.0001	0.6694± 0.0051	$w=-1$
wCDM	0.3163± 0.0081	0.0223± 0.0015	0.6717± 0.0074	w=-0.9927± 0.0268
CPL	0.3134± 0.0062	0.0222± 0.0001	0.6752± 0.0046	w=-0.9996± 0.0008 wa=-0.0284± 0.0013
β-model	0.3139± 0.0082	0.0222± 0.0001	0.6749± 0.0088	β_0=2.0128± 0.0542

where $H(z)$ is the Hubble parameter in terms of redshift z and H_0 is the current value of the Hubble constant. The matter density parameter is denoted by $\Omega_m(z) = \Omega^0_m(1+z)^3$, $\Omega_{rad}(z) = \Omega^0_{rad}(1+z)^4$ and the term $\Omega_{ext}(z) = \Omega^0_{ext}(1+z)^{4-2\beta_0}\gamma_0$ stands for the density parameter associated with the extrinsic curvature. The current extrinsic contribution Ω^0_{ext} is given by the normalization condition for redshift at $z = 0$ that results in

$$\Omega^0_{ext} = \gamma_0 \left(1 - \Omega^0_m - \Omega^0_{rad}\right) . \tag{22}$$

Hence, we can write the dimensionless Hubble parameter $E(z)$ as

$$E^2(z) = \Omega^0_m(1+z)^3 + \Omega^0_{rad}(1+z)^4 + \left(1 - \Omega^0_m - \Omega^0_{rad}\right)(1+z)^{4-2\beta_0} , \tag{23}$$

Hereon, the present model is denoted as β-model to facilitate the referencing.

B. Results

We compare our results with three phenomenological models to ascertain how the β-model is constrained to available data and the related σ-distance. In table I and II, we present the best-fit values and mean values the studied model. In figures 1 and 2, the comparisons are made with the models from left-to-right sequence. In all cases, the lower panel indicates the comparison between CPL and β-model.

In figures, we perform the σ-contours with $68,3\%$, $95,4\%$ and $99,7\%$ confidence levels (C.L.) in the $(\beta - \Omega_m)$ and $(\Omega_b h^2 - \Omega_m)$ 2-d planes, respectively. The black points denote the mean values of the β-model and red points refer to the models in comparison. To start the analysis, we use an initial reference on the σ-distances between the models, a higher distance means a higher tension between models in question. The σ-distances D_σ can be computed by

$$D_\sigma = \sqrt{2}\, Inverf\left[0, 1 - \Gamma(1, \frac{\Delta\chi^2}{2})\right] , \tag{24}$$

where $Inverf(x)$ is the inverse of the error function $Erf(x)$ and $\Gamma(1, \frac{\Delta\chi^2}{2})$ is the incomplete gamma function, with $\Delta\chi^2 = \chi^2_{model\ (2)} - \chi^2_{model\ (1)}$. The resulting differences between points in figure 1 were the comparisons $(\beta - \Lambda\text{CDM})$ with 0.04σ, $(\beta - w\text{CDM})$ and $(\beta\text{-CPL})$ with 0.13σ, 0.06σ, respectively. These results lead to a close equivalence between the models favoring the β model closer to ΛCDM with a smaller σ-distance. More importantly, the obtained distances are much smaller than 1-σ, which is a symptom of a statistically concordance models.

A more solid statistical reference can be made with AIC and BIC classifiers. Firstly, we adopt the errors from the data being as Gaussian and use AIC to evaluate the fit-to-data for small samples sizes [62, 63] by the formula

$$AIC = \chi^2_{bf} + 2k\frac{2k(k+1)}{N-k-1} , \tag{25}$$

where χ^2_{bf} is the best fit χ^2 of the model, k represents the number of the uncorrelated (free) parameters and N is the number of the data point in the adopted dataset. The difference $|\Delta AIC| = AIC_{model\ (2)} - AIC_{model\ (1)}$ obeys the Jeffreys' scale [64] that measures the intensity of tension between two models, i.e., higher values for $|\Delta AIC|$ denotes more tension between models and more statistically uncorrelated they are. For $|\Delta AIC \leq 2|$ the models are statistically consistent and equivalents. For $4 < \Delta AIC < 7$ and $|\Delta AIC \geq 10|$ induces to growing tension between the models with positive evidence and strong evidence against the equivalence of the models, respectively. Accordingly, we have obtained for the first

Preprints (www.preprints.org) | NOT PEER-REVIEWED | Posted: 8 May 2019 doi:10.20944/preprints201905.0096.v1

TABLE III. A summary of the obtained values of AIC and BIC for the studied models.

Model	AIC	ΔAIC	BIC	ΔBIC
ΛCDM	1817.71	0.07	1837.67	0.07
wCDM	1817.85	0.21	1837.81	0.21
CPL	1819.75	2.11	1844.69	7.09
β-model	1817.64	0	1837.60	0

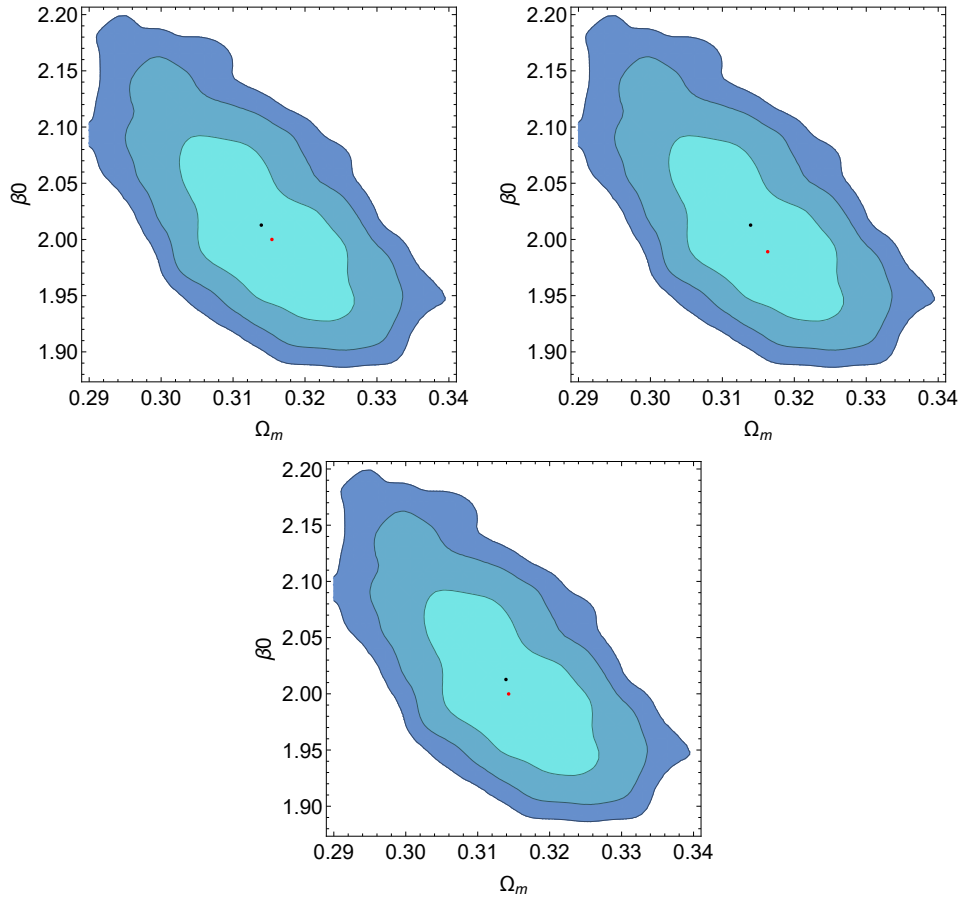

FIG. 1. Contour regions at 1-σ, 2-σ and 3-σ with $68,3\%$, $95,4\%$ and $99,7\%$ C.L., respectively, in the plane $(\beta_0 - \Omega_m)$. The black points represents the mean values of the parameters in the MCMC chain. The red dots denote the β-model and the black dots denote the comparison models and from left-to-right, we have ΛCDM, wCDM and CPL (lower panel) models.

case (β-ΛCDM) a value 0.07, and for ($\beta - w$CDM) and (β-CPL), the values 0.21 and 2.11, respectively. This result leads to the same conclusion: the β-model favors more ΛCDM with smaller values of AIC, even though the β-model is statistically consistent also with wCDM and CPL models that represents dynamical DE models.

Likewise, we apply BIC classifiers [54] that work well for independent homogeneous distribution of datasets [62]. Unlike AIC, the BIC method heavily penalizes free parameters of a model. To check this out, we use the following formula

$$BIC = \chi^2_{bf} + k \ln N \,, \tag{26}$$

where χ^2_{bf} is the best fit χ^2 of the model, k represents the number of the uncorrelated (free) parameters and N is the number of the data point in the adopted dataset. Therefore, from Jeffreys' scale, a smaller BIC values favor statistically better models (lower tension between two comparison models). In these terms, we have similar results as those obtained from AIC, expect for the case (β-CPL) which in BIC analysis it has roughly a BIC value ~ 7 indicating a positive tension between the models. This is the fact that CPL model has an additional free parameter and BIC analysis is severe on free parameters. Since we have fixed our analysis on late transition redshifts that implies in $\eta_0 = 0$, this tension may be alleviated if we let the η_0 parameter runs freely. The table (III) shows a summary of AIC and BIC values for the models.

Preprints (www.preprints.org) | NOT PEER-REVIEWED | Posted: 8 May 2019 doi:10.20944/preprints201905.0096.v1

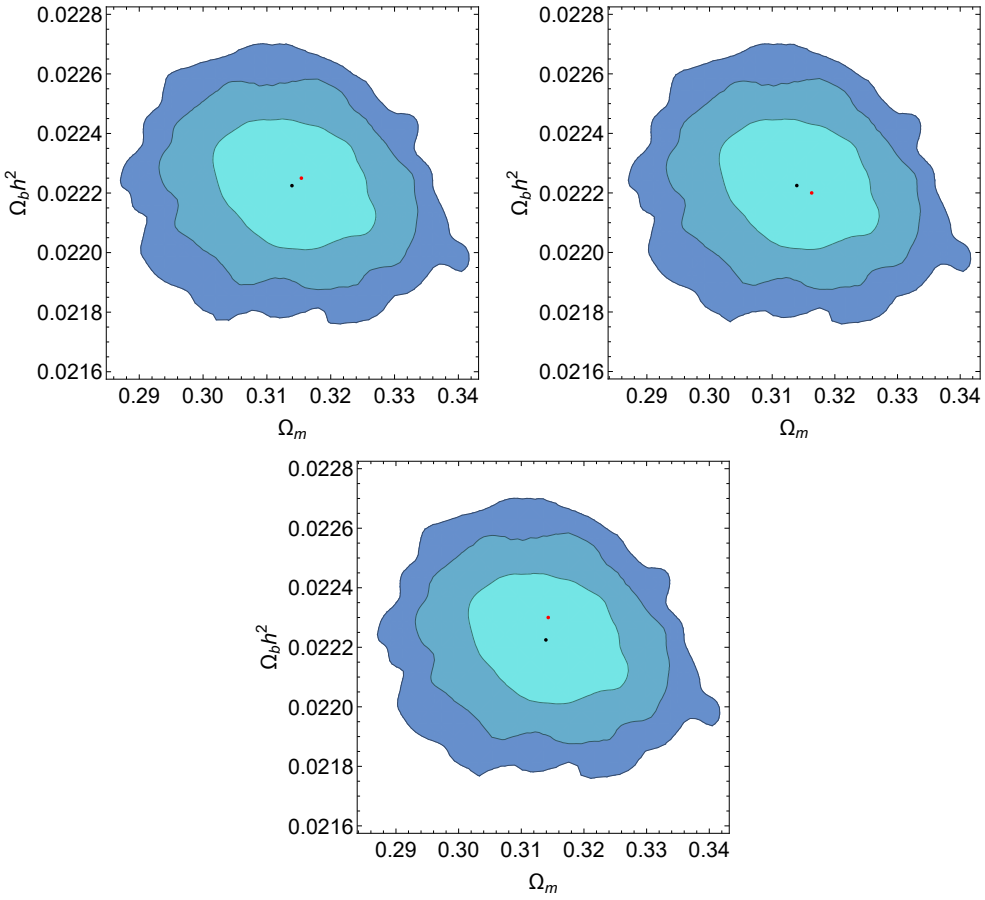

FIG. 2. Contour regions at 1-σ, 2-σ and 3-σ with $68,3\%$, $95,4\%$ and $99,7\%$ C.L., respectively, in the plane $(\beta_0 - \Omega_b h^2)$. The points represents the mean values of the parameters in the MCMC chain. The red dots denote the β-model and the black dots denote the comparison models and from left-to-right, we have ΛCDM, wCDM and CPL (lower panel) models.

IV. REMARKS

In this paper, we have discussed the dark energy problem with a proposal of a geometric model based on the Nash-Green embedding theorem. Using the corresponding modified Friedman equation in a flat background, we confronted the present model to popular models like ΛCDM, wCDM and CPL through a joint analysis on recent datasets (Pantheon, CBM, BAO and $H(z)$). Focusing on late transition with redshift fixed at z=1, the model loses a free parameter η_0 since it is inner related to the transition redshift. We found that the studied models are statistically indistinguishable at 1-σ C.L. with the AIC values roughly 2. The σ-distances are smaller than 0.5-σ between the mean values calculated from a MCMC method and the best-fit values for 1-σ C.L. for the other models. We also tested the tension between the models using the BIC criterion and found results as much as similar to AIC, with exception for the CPL model. In this case, we found a BIC values around 7 that represents a positive tension between the models due to the fact that the CPL model has a additional free parameter, and BIC method penalizes more provoking more tension between models. An overall conclusion, we have a model that favors ΛCDM with a mild deviation and we did not identified at any place a phantom behaviour. As future prospects, we intend to investigate the evolution of the background with the evaluation of the evolution equations of the perturbations in order to confront the behaviour of the viscosity parameter and growth index rate. This process is in due course and will be reported elsewhere.

ACKNOWLEDGMENTS

The author thanks Federal University of Latin-American Integration for financial support from Edital PRPPG 110 (17/09/2018) and Fundação Araucária/PR for the Grant CP15/2017-P&D 67/2019.

[1] R. J. Nemiroff, R. Joshi, B.R. Atla, JCAP06, 006, (2015).
[2] B. Santos, A. A. Coley, N. Chandrachani Devi, J. S. Alcaniz, JCAP02, 047, (2017).
[3] P. Kumar, C.P. Singh, Astrophys Space Sci., 362, 52, (2017).
[4] H.E.S. Velten, R.F. vom Marttens, W. Zimdahl, Eur.Phys.J. C74, 11, 3160, (2014).
[5] J. Sultana, Mon.Not.Roy.Astron.Soc. 457(1), 212-216, (2016).
[6] N. Sivanandam, Phys. Rev. D 87, 083514, (2013).
[7] K. Nozari, N. Behrouz and N. Rashidi, Advances in High Energy Physics, Article ID 569702 2014, (2014).
[8] P. A. R. Ade et al. (Planck), Astron. Astrophys. 594, A13, (2016).
[9] N. Arkani-Hamed et al, Phys. Lett., B429, 263, (1998).
[10] L. Randall, R. Sundrum, Phys. Rev. Lett., 83, 3370,(1999).
[11] L. Randall, R. Sundrum, Phys. Rev. Lett., 83, 4690, (1999).
[12] G. Dvali, G. Gabadadze, M. Porrati, Phys. Lett.B485, 1-3, 208-214, (2000).
[13] R. A. Battye, B. Carter, Phys. Lett. B, 509, 331, (2001).
[14] M.D. Maia, E.M. Monte, Phys. Lett. A, 297, 2, 9-19, (2002).
[15] M.D. Maia, E.M. Monte, J.M.F. Maia, J.S. Alcaniz, Class.Quantum Grav., 22, 1623, (2005).
[16] M.D. Maia, N. Silva, M.C.B. Fernandes, JHEP, 04, 047, (2007).
[17] M. Heydari-Fard, H. R. Sepangi, Phys.Lett., B649, 1-11, (2007).
[18] S. Jalalzadeh, M. Mehrnia, H. R. Sepangi, Class.Quant.Grav., 26,155007, (2009).
[19] M.D. Maia, A.J.S Capistrano, J.S. Alcaniz, E.M. Monte, Gen. Rel. Grav., 10, 2685, (2011).
[20] A. Ranjbar, H.R. Sepangi, S. Shahidi, Ann. Phys., 327, 3170-3181, (2012).
[21] A. J. S. Capistrano, L.A. Cabral, Ann. Phys., 384, 64-83, (2014).
[22] A. J. S. Capistrano, Montl. Not. Roy. Soc, 448, 1232-1239, (2015).
[23] A. J. S. Capistrano, L. A. Cabral, Class. Quantum Grav. 33, 245006, (2016).
[24] A. J. S. Capistrano, A. C. Gutirrez-Pieres, S. C. Ulhoa, R. G.G. Amorim, Ann. Phys., 380, 106120, (2017).
[25] A. J. S. Capistrano, Ann. Phys. (Berlin), 1700232, (2017).
[26] C. T. Hill, D. N. Schramm, J. N. Fry, Comments Nucl. Part. Phys., 19, 25, 407, (1988).
[27] A. B. Bassett, M. Kunz, J. Silk, C. Ungarelli, Mon. Not. R. Astron. Soc. 336, 1217-1222, (2002).
[28] L. Parker, A. Raval, Phys. Rev., D60, 123502, 1999 [Erratum: Phys. Rev.D67,029902(2003).
[29] L. Parker, A. Raval, Phys. Rev., D62, 083503, 2000 [Erratum: Phys. Rev.D67,029903(2003)]
[30] M. J. Mortonson, W. Hu, D. Huterer, Phys. Rev., D80, 067301, (2009).
[31] E. Di Valentino, E. V. Linder, A. Melchiorri, Phys. Rev., D97, 043528, (2018).
[32] J.-B. Durrive, J. Ooba, K. Ichiki, N. Sugiyama, Phys. Rev., D97, 043503, (2018).
[33] C. J. A. P. Martins, M. Prat Colomer. A&A 616, A32, (2018).
[34] C. A. Luna, S. Basilakos, S. Nesseris, Phys. Rev. D 98, 023516, (2018).
[35] R. Arjona, W. Cardona, S. Nesseris, Phys. Rev. D 99, 043516, (2019).
[36] D. M. Scolnic et al., Astrophys. J. 859, 101 (2018), 1710.00845.
[37] C. Zhang, H. Zhang, S. Yuan, T.J. Zhang, and Y.-C. Sun, Res. Astron. Astrophys. 14, 1221, (2014), 1207.4541.
[38] D. Stern, R. Jimenez, L. Verde, M. Kamionkowski, and S. A. Stanford, JCAP 1002, 008, (2010).
[39] M. Moresco et al., JCAP 1208, 006, (2012).
[40] C.H. Chuang and Y. Wang, Mon. Not. Roy. Astron. Soc. 435, 255, (2013).
[41] M. Moresco, Mon. Not. Roy. Astron. Soc. 450, L16, (2015).
[42] T. Delubac et al. (BOSS), Astron. Astrophys. 574, A59, (2015).
[43] F. Beutler, C. Blake, M. Colless, D. H. Jones, L. Staveley-Smith, L. Campbell, Q. Parker, W. Saunders, and F. Watson, Mon. Not. Roy. Astron. Soc. 416, 3017, (2011).
[44] L. Anderson et al. (BOSS), Mon. Not. Roy. Astron. Soc.441, 24, (2014).
[45] X. Xu, N. Padmanabhan, D. J. Eisenstein, K. T. Mehta,and A. J. Cuesta, Mon. Not. Roy. Astron. Soc. 427, 2146, (2012).
[46] C. Blake et al., Mon. Not. Roy. Astron. Soc. 425, 405, (2012).
[47] A. J. Ross, L. Samushia, C. Howlett, W. J. Percival,A. Burden, and M. Manera, Mon. Not. Roy. Astron.Soc. 449, 835 (2015), 1409.3242.
[48] H. Gil-Marín et al., Mon. Not. Roy. Astron. Soc. 460, 4210, (2016).
[49] R.R. Caldwell, R. Dave, P.J. Steinhardt, Phys. Rev. Lett. 80, 1582, (1998).
[50] B. Ratra, P. J. E. Peebles, Phys. Rev. D 37, 3406, (1988).
[51] M. Chevallier, D. Polarski, Int. J. Mod. Phys. D 10, 213, (2001).
[52] E. V. Linder, Phys. Rev. Lett., 90, 091301, (2003).
[53] H. Akaike, IEEE Transactions of Automatic Control, 19, 716, (1974).
[54] G. Schwarz, Ann. Statist., 5, 461, (1978).
[55] S. K. Donaldson, Contemporary Mathematics (AMS), 35, 201, (1984).
[56] C. H. Taubes, Contemporary Mathematics (AMS), 35, 493, (1984).
[57] C.S. Lim, Prog. Theor. Exp. Phys., 02A101, (2014).
[58] J. Nash, Ann. Maths., 63, 20, (1956).
[59] R. Greene, Memoirs Amer. Math. Soc., 97, (1970).
[60] S.N. Gupta, Phys. Rev., 96, 6, (1954).
[61] M.S. Turner, M. White, Phys. Rev. D56, 4439, (1987).
[62] A. R. Liddle, Mon. Not. R. Astron. Soc. 377, L74L78, (2007).
[63] N. Sugiura, Communications in Statistics A, Theory and Methods, 7, 13, (1978).
[64] H. Jeffreys, Theory of Probability, 3rd edn. Oxford Univ. Press, Oxford, (1961).